Materials Today Communications 26 (2021) 101823

Contents lists available at ScienceDirect

Materials Today Communications

journal homepage: www.elsevier.com/locate/mtcomm

Computational study of metal doped graphene nanoribbon as a potential platform for detection of H_2S

Ehab Salih [a], Ahmad I. Ayesh [b,*]

[a] Department of Mathematics, Statistics and Physics, Qatar University, P. O. Box 2713, Doha, Qatar
[b] Center for Sustainable Development, Qatar University, P. O. Box 2713, Doha, Qatar

ARTICLE INFO

Keywords:
Graphene
Gas sensor
H_2S adsorption
Pt doping
Armchair graphene nanoribbon

ABSTRACT

Theoretical investigation for detection of hydrogen sulfide (H_2S) gas using hydrogen/nitrogen-terminated armchair graphene nanoribbon (HAGNR and NAGNR) doped with Pt is presented in this study. The investigation was established with the aid of Atomistic ToolKit Virtual NanoLab (ATK-VNL) that employs density functional theory (DFT) computations. The results revealed that NAGNR has a higher adsorption energy (E_{ads}) of −0.369 eV, smaller adsorption length (l) of 3.08 Å, and higher charge transfer (Δq) of −0.034 e than the HAGNR system. The adsorption parameters, and hence the sensitivity, of the two presented HAGNR and NAGNR systems were improved by doping the nanoribbon with Pt. More precisely, E_{ads} increased remarkably to almost 13 and 10 times for the cases of HAGNR-Pt and NAGNR-Pt as compared with bare HAGNR and NAGNR, respectively. To further confirm the effect of doping with Pt on the performance of HAGNR and NAGNR, the sensitivity of gas sensor devices was studied by calculating the response of H_2S for the developed HAGNR, NAGNR, HAGNR-Pt, and NAGNR-Pt systems. Interestingly, the response towards H_2S increased considerably to 46.7 and 40.0 % for the cases HAGNR-Pt and NAGNR-Pt, respectively. Finally, the obtained results in the current study demonstrate that both HAGNR-Pt and NAGNR-Pt successfully adsorbed the H_2S gas with enhanced sensitivity.

1. Introduction

Hydrogen sulfide (H_2S) is a considerably poisonous, highly explosive, and colorless gas that is characterized by the smell of rotten egg at low concentration [1]. H_2S is mostly associated with the various petrochemical and other manufacturing processes such as natural gas treatment [2–4]. Exposure to H_2S has extremely serious influences on the nervous as well as the respiratory systems of humans [5]. More precisely, breathing H_2S may results in cough and runny nose at low concentration, while breathing high concentrations could lead to coma and pulmonary edema [6,7]. Consequently, developing a sensitive gas sensor to early detect the toxic H_2S gas even at low concentrations is extremely important to protect the health of human beings [8,9].

The detection of H_2S gas has been widely investigated experimentally as well as theoretically using graphene based nanomaterials (GNMs) in the recent decade. For example, Ovsianytskyi et al. designed a sensor for sensitive and selective detection of H_2S using graphene (G) decorated with silver nanoparticles (Ag-NPs) as well as charged impurities [10]. Their results demonstrated that decorating G improved remarkably its sensitivity as well as selectivity to H_2S gas. Reduced graphene oxide-loaded $ZnFe_2O_4$ nanofibers based gas sensor has been also fabricated and then used to detect H_2S by Hoang et al. [11]. The results of this study reflected an improvement on the sensing performance due to the presence of the nanofibers. Song and coworkers investigated a highly sensitive H_2S gas sensor using reduced graphene oxide modified with SnO_2 quantum wires [12]. The researchers of this study showed that the developed sensor reflected an excellent sensing performance thanks to the improved electron transport as a result of the favorable charge transfer of SnO_2-reduced graphene oxide interfaces [12]. A theoretical study on the detection of CO, CO_2, SO_2 and H_2S gases based on intrinsic as well as Fe-doped graphene was investigated by Cortés-Arriagada and coworkers [13]. They demonstrated in this study that the performance of Fe-doped graphene remarkably enhanced after doping with Fe. Gao et al. compared between the adsorption of H_2S as well as CH_4 gases using pure graphene and Ni, vacancy, and −OH modified graphene [14]. They demonstrated a considerable improvement in the adsorption parameters as a result of graphene modification. In another study, the detection of NO_2 as well as H_2S gases with the aid of pure and metal decorated graphene has been done by Bo and coworkers [15]. The researchers in this study showed that decorating

* Corresponding author at: Center for Sustainable Development, Qatar University, P. O. Box 2713, Doha, Qatar.
E-mail address: ayesh@qu.edu.qa (A.I. Ayesh).

https://doi.org/10.1016/j.mtcomm.2020.101823
Received 28 July 2020; Received in revised form 3 October 2020; Accepted 19 October 2020
Available online 2 November 2020

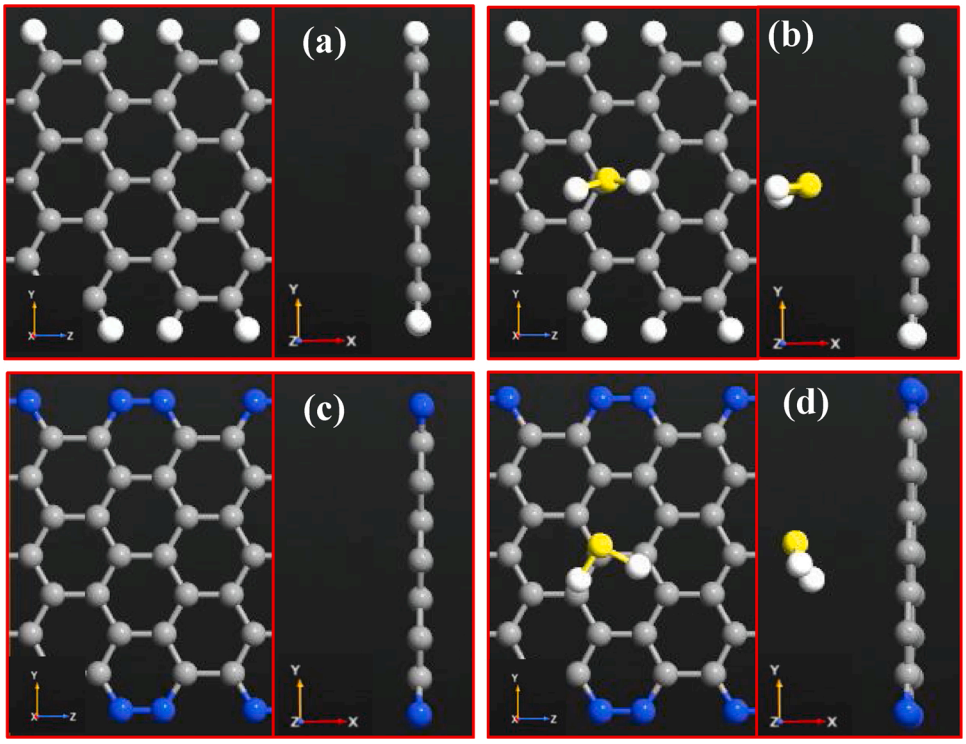

Fig. 1. Tope and side views of the relaxed a) HAGNR, b) HAGNR-H_2S, c) NAGNR, and d) NAGNR-H_2S.

graphene with Ni, Pa, and Pt lead to enhancing the sensing performance. Specifically, they found that after decorating graphene, the adsorption energy increased 7–10 times as compared with the pristine graphene [15]. Based on the above-mentioned reports, one can conclude that doping as well as decorating graphene based materials with different metals and metal oxides could lead to magnificent accomplishments in the gas sensor applications [16–18].

Moreover, it has been reported that the influence of gas adsorption on the electronic features of zero band gap materials is not considerable as compared with the materials that exhibit a small band gap [19]. Therefore, AGNR was considered as the platform of this study thanks to its enormous surface area to volume ratio, the presence of edge bonds as well as the ability to control its band gap [20,21].

Herein, the sensing performance of H_2S using hydrogen/nitrogen-terminated and Pt-doped armchair graphene nanoribbon (HAGNR, NAGNR, HAGNR-Pt, and NAGNR-Pt) systems has been investigated theoretically. The obtained results showed that H_2S adsorbed on N-terminated AGNR has a slightly higher adsorption energy as well as charge transfer when compared with the H-terminated AGNR. The sensitivity of the two developed HAGNR and NAGNR systems was improved via doping with Pt metal. The adsorption energy increased considerably to almost 13 times for the case H_2S adsorbed on HAGNR-Pt and 10 times for the case of H_2S adsorbed on NAGNR-Pt. Specifying that doping both HAGNR and NAGNR with Pt is crucial to modify their performance to detect H_2S gas.

2. Simulation methods

The effects of terminating AGNR with hydrogen and nitrogen as well as doping with Pt on the adsorption capability toward the toxic H_2S gas were studied using density functional theory (DFT) [22]. The generalized gradient approximation (GGA) was used as the processing method as described by Perdew–Burke–Ernzerhof (PBE) with the implementation of DFT-D2 proposed by Grimme to treat Van der Waals interactions to correct for underestimation of band gap by GGA [23,24]. Nevertheless, no focus on dispersion of calculations of the non-chemically-bonded Van der Waals interactions. The geometry optimization of H_2S adsorbed on all the proposed sensor materials to assure true local minima was considered using the LBFGS optimizer [25]. Hence, all the systems have been relaxed until a residual force per atom lower than 0.05 eV/Å was obtained. A Pack k point sampling of $4 \times 4 \times 1$ was considered for the four systems, while for the current-voltage (I(V)) investigations k-point sampling of $1 \times 1 \times 100$ was used. A 125 Hartree and 0.01 GPa have been considered as the density mesh cutoff and the stress error tolerance, respectively.

For a better evaluation of the interaction between the H_2S gas and the developed HAGNR, NAGNR, HAGNR-Pt, and NAGNR-Pt systems, the adsorption energies were calculated using Eq. (1) [26–29]:

$$E_{ads} = E_{H/N-AGNR/Pt+H_2S} - E_{H/N-AGNR/Pt} - E_{H_2S} \quad (1)$$

Where $E_{H/N-AGNR/Pt+H_2S}$ and $E_{H/N-AGNR/Pt}$ represent the total energies of any of the developed systems with and without the H_2S gas, respectively. While, E_{H_2S} represents the total energy of the toxic H_2S molecule. To further confirm the adsorption of H_2S on any of the built systems, the charge transfer of H_2S gas has been elaborated using Eq. (2) [30]:

$$\Delta q = q_a - q_b \quad (2)$$

Where Δq corresponds to the charge transfer of H_2S, while q_a and q_b refer to Mulliken charges of the toxic H_2S gas after and before, respectively, the interaction with any of the proposed sensor materials. Mulliken population method was used to explore the charge transfer due to its widespread usage upon performing the calculations employing LCAO basis sets [31].

3. Results and discussion

AGNR is considered in the present work as a computational platform for gas sensor to detect H_2S gas. AGNR is firstly passivated with either hydrogen or nitrogen generating two systems (HAGNR and NAGNR) to satisfy the dangling bonds and to avoid the edge reconstruction [32]. The relaxed structures of both HAGNR and NAGNR systems with and

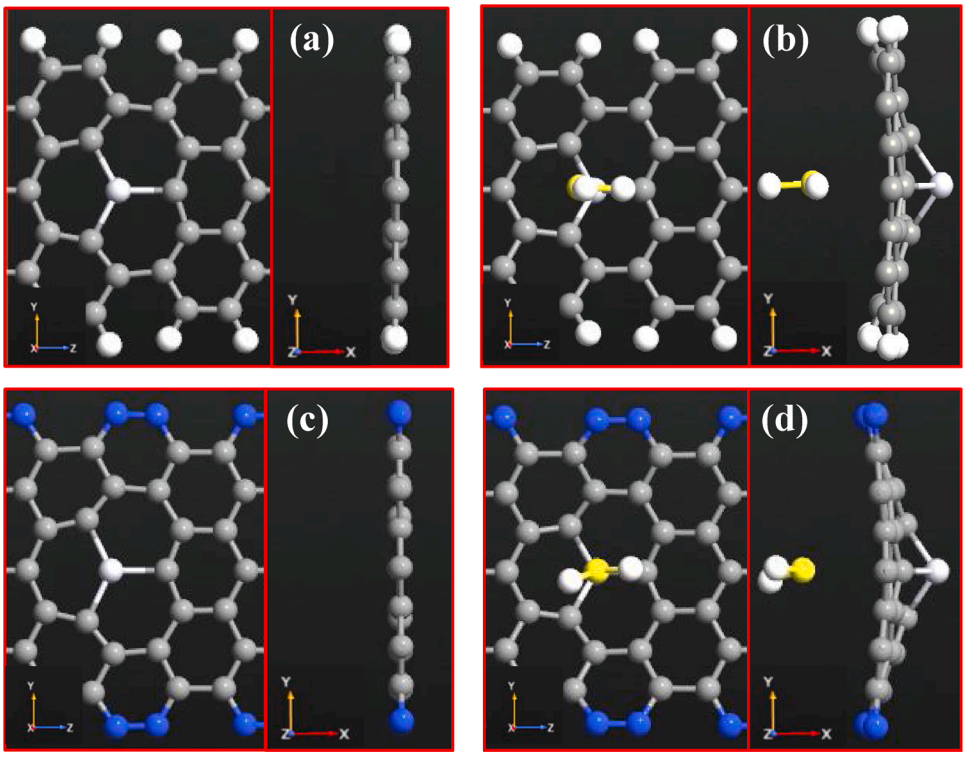

Fig. 2. Tope and side views of the relaxed a) HAGNR-Pt, b) HAGNR-Pt-H_2S, c) NAGNR-Pt, and d) NAGNR-Pt-H_2S.

Table 1
Adsorption energy (E_{ads}), adsorption length (l), and charge transfer (Δq) of HAGNR-H_2S, NAGNR-H_2S, HAGNR-Pt-H_2S, and NAGNR-Pt- H_2S.

System	E_{ads} (eV)	l (Å)	Δq (e)
HAGNR-H_2S	−0.301	3.40	−0.024
NAGNR-H_2S	−0.369	3.08	−0.034
HAGNR-Pt-H_2S	−4.115	2.93	0.037
NAGNR-Pt-H_2S	−3.892	3.47	−0.042

without gas are shown in Fig. 1(a)–(d). Upon optimization, the results reflect that the lengths of the C—C bond are 1.44 and 1.43 Å for the cases of HAGNR and NAGNR, respectively. Fig. 1(b) and (d) show that H_2S gas reorients itself to attain the best stable configuration wherein the sulfur atom of H_2S becomes closer to the plane of the HAGNR system than the two hydrogen atoms. In contrast, the two hydrogen atoms face the plane of the ribbon for the case of NAGNR upon optimization. In order to enhance the adsorption parameters and hence the sensitivity, the two built HAGNR and NAGNR systems are doped with Pt in which a single carbon atom in the ribbon is replaced with a Pt atom generating two more systems (HAGNR-Pt and NAGNR-Pt). Subsequently, a stress is generated in the systems by the Pt atom [33]. The systems then experience some changes in the lengths of C-Pt bonds to release this stress. Specifically, the bonds around the Pt atoms expand to 1.79 and 1.83 Å for the cases of HAGNR-Pt and NAGNR-Pt, respectively. As described in Fig. 2(b) and (d), the Pt atom is pulled down the plan of the ribbon after the interaction with the gas which results in further extension of the lengths of bonds around Pt atom to 1.96 and 1.95 Å for the cases of HAGNR-Pt and NAGNR-Pt, respectively. Meanwhile, the configuration with the sulfur atom and one hydrogen atom facing HAGNR-Pt, and only the sulfur atom facing NAGNR-Pt are found to be the preferable ones after relaxation.

To evaluate the sensing performance of the four sensor systems HAGNR, NAGNR, HAGNR-Pt, and NAGNR-Pt toward the detection of H_2S gas, the adsorption energy E_{ads}, adsorption length l, as well as the charge transfer Δq are investigated. The results reflect that the adsorption energy and the charge transfer between the gas and the built sensors are −0.301 eV and −0.024 e for the case of HAGNR, and −0.369 eV and -0.034 e for the case of NAGNR as shown in Table 1. The obtained adsorption energies for both HAGNR and NAGNR are almost 3 folds higher than the case of pure AGNR that has been reported recently [34]. Meanwhile, the smallest direct distances between the gas molecules and the systems are 3.40 and 3.08 Å for the cases of HAGNR and NAGNR, respectively. Furthermore, the charge transfer analysis shows that electrons transfer from the system to the gas in the two cases. Based on the adsorption parameters, one can say that NAGNR is more preferable for the detection of H_2S gas. The sensing performance of the built materials toward H_2S is improved remarkably after doping with Pt. More precisely, the adsorption energies increase significantly to −4.115 and −3.892 eV for the cases of HAGNR-Pt and NAGNR-Pt, respectively. In addition, the Mulliken population analysis shows that 0.037 e transfer from HAGNR-Pt to the H_2S gas, while 0.042 e transfer from the gas to NAGNR-Pt. Meanwhile, the adsorption lengths between H_2S and HAGNR-Pt and NAGNR-Pt are found to be 2.93 and 3.47 Å, respectively. The obtained results of the adsorption energy after doping the built systems with Pt indicates that the adsorption of H_2S gas on the surface of both HAGNR-Pt and NAGNR-Pt is chemisorption, while it is physisorption for the cases of HAGNR and NAGNR [35–37].

The band structures of HAGNR, NAGNR, HAGNR-Pt, and NAGNR-Pt with and without the H_2S gas are investigated as shown in Figs. 3 and 4. The results demonstrate a parabolic trend around the Γ point for both HAGNR and NAGNR as described in Fig. 3(a) and (b). After adsorption of H_2S on HAGNR and NAGNR (Fig. 3(c) and (d)), no considerable changes are detected at the Fermi level. Nevertheless, some variations appear near Fermi level between −1.0 and −2.0 eV in the valence band. Fig. 4 (a)–(d) show the band structures of HAGNR-Pt and NAGNR-Pt with and without the gas. Fig. 4(a) shows that some new bands are observed in the valence as well as the conduction bands of HAGNR-Pt when compared with HAGNR. The same behavior is detected as well for the case of NAGNR-Pt (Fig. 4(b)) in addition to the movement of the valence and the conduction bands away from Fermi level. As a result of H_2S adsorption on both HAGNR-Pt and NAGNR-Pt, considerable changes as

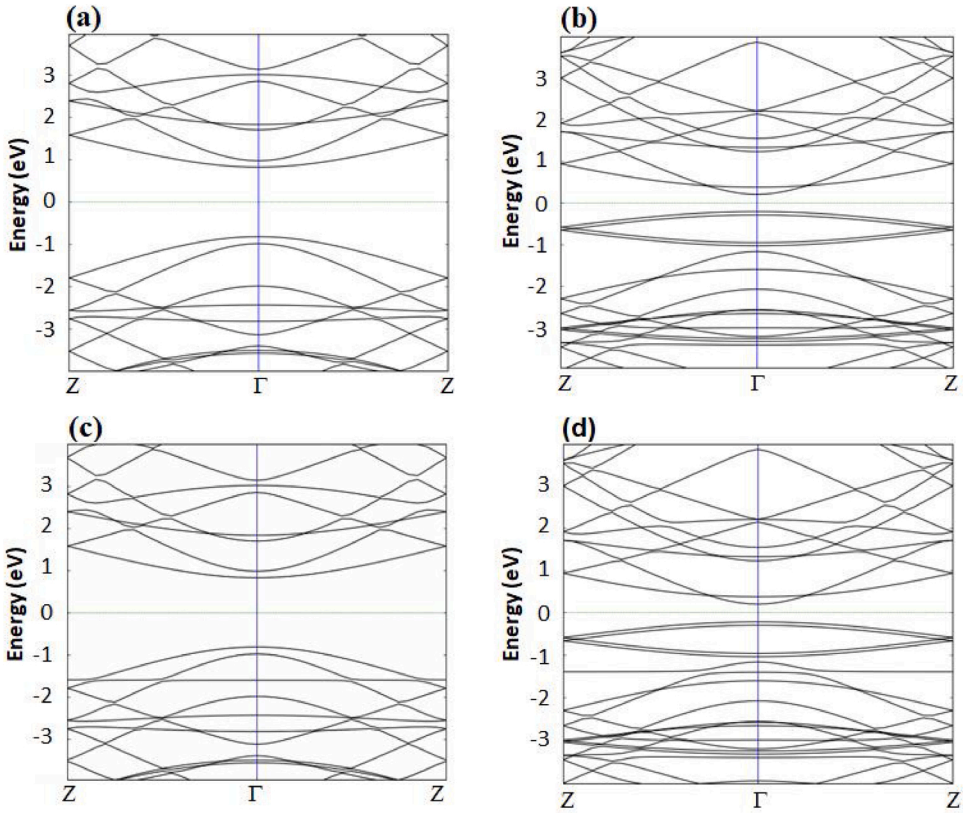

Fig. 3. Band structures of a) HAGNR, b) NAGNR, c) HAGNR-H_2S, and d) NAGNR-H_2S.

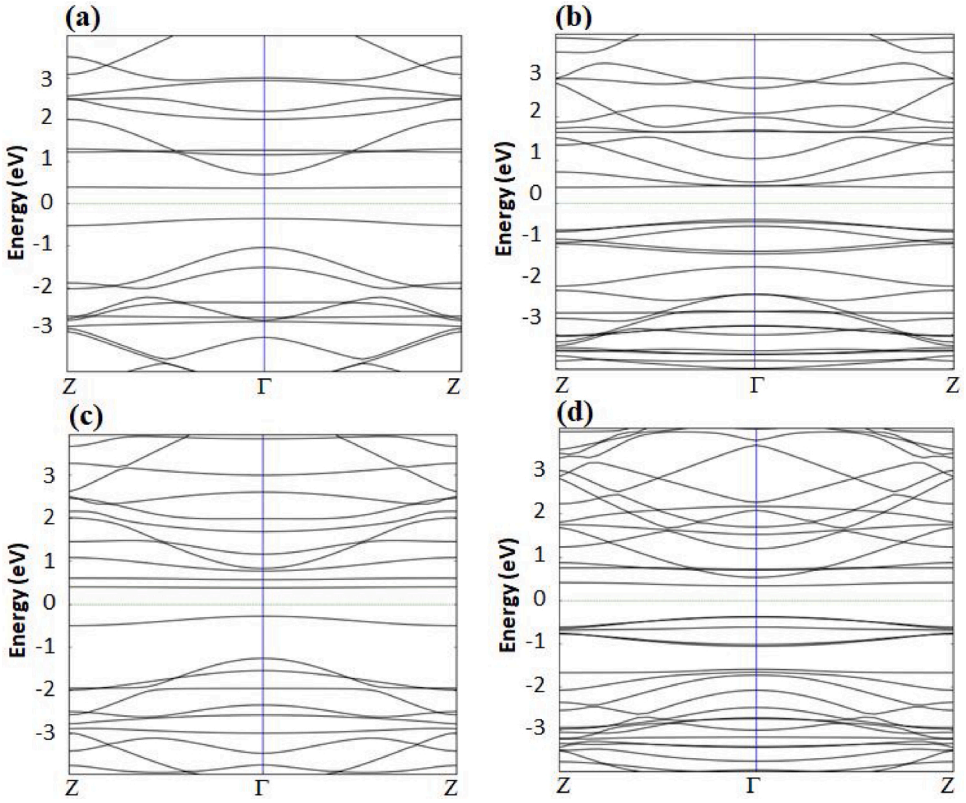

Fig. 4. Band structures of a) HAGNR-Pt, b) NAGNR-Pt, c) HAGNR-Pt-H_2S, and d) NAGNR-Pt-H_2S.

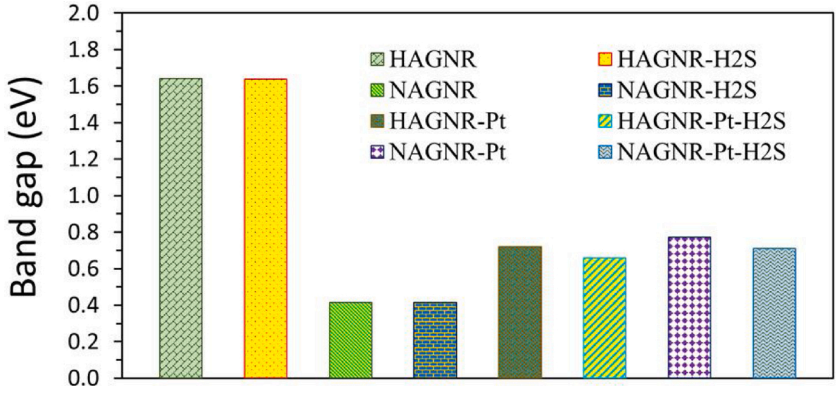

Fig. 5. Band gaps of HAGNR, NAGNR, HAGNR-Pt, and NAGNR-Pt with and without the gas.

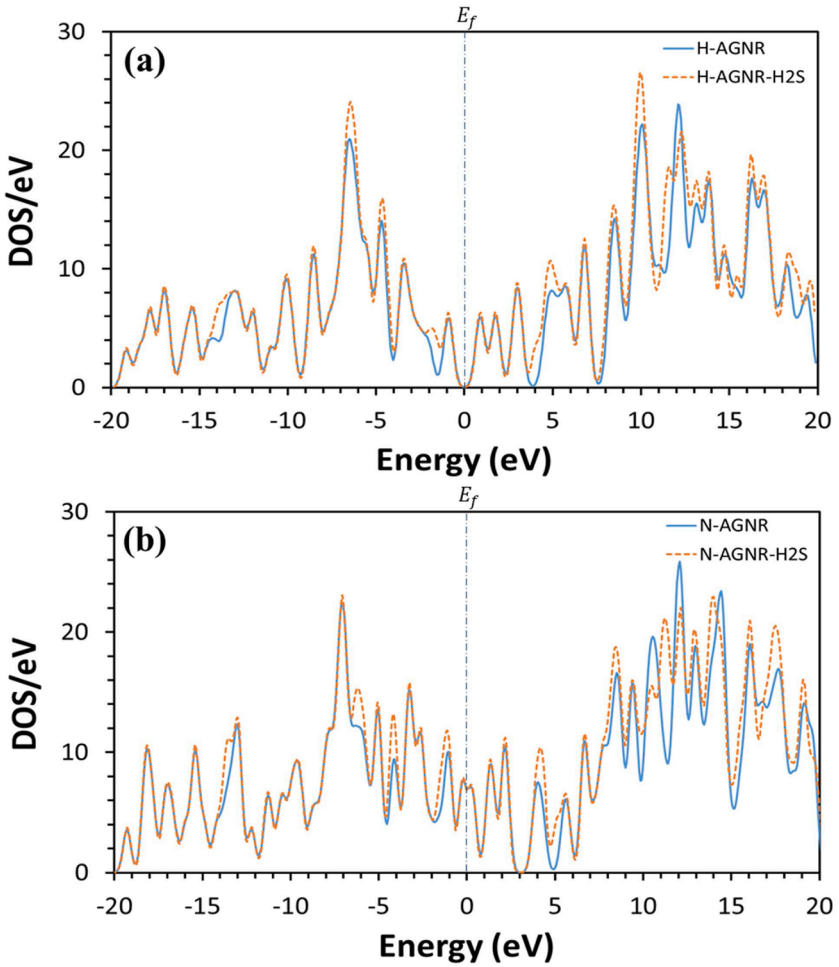

Fig. 6. Total electronic density of states of a) HAGNR, and b) NAGNR with and without the H_2S gas.

well as new bands are detected in the valence and conduction bands as shown in Fig. 4(c) and (d). Furthermore, the direct band gaps at the Γ point of the developed sensors with and without the gas are measured as shown in Fig. 5. It is worth noting that there are no significant changes observed in the band gaps upon the adsorption of H_2S on HAGNR and NAGNR systems. Upon adsorption of H_2S on the surface of HAGNR-Pt and NAGNR-Pt, the band gaps decrease to 0.66 and 0.71 eV, respectively. As clearly demonstrated, the adsorption of H_2S showed noticeable variations on the electronic properties only for the cases of HAGNR-Pt and NAGNR-Pt. The variations and new bands in the valence as well as conduction bands, observed after gas adsorption, are mostly an indication of the formation of new electronic states upon the adsorption of H_2S [38]. These results of band structures suggest that those systems can be utilized for successful adsorption of H_2S gas.

To further confirm the influence of adsorption of H_2S on the electronic characteristics of the built systems, the electronic density of states (DOS) of the proposed sensors with and without the gas are investigated. Fig. 6(a) and (b) show the DOS of the developed HAGNR and NAGNR sensors with and without the gas. For the case of HAGNR (Fig. 6(a)), the DOS in the ranges of −6.4 to −1.8 eV and 4.9–19.6 eV increases after adsorption of H_2S. While changes are observed in the ranges of −6.1 to −1.1 eV in the valence band and 4.3–19.1 eV in the conduction band

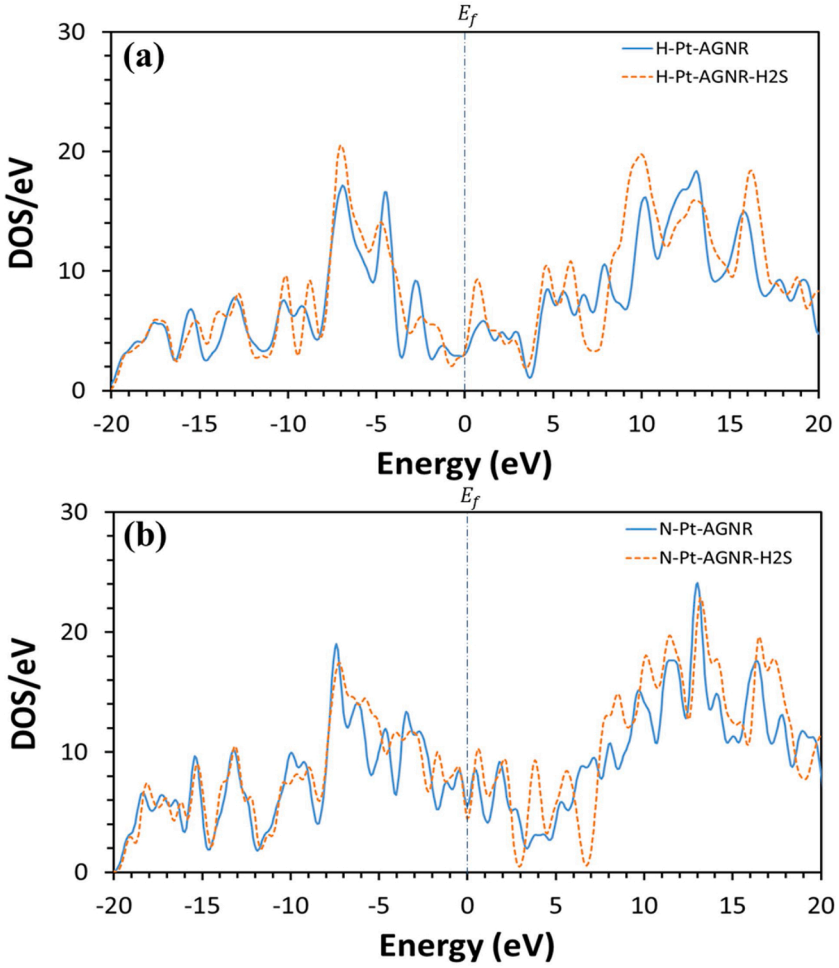

Fig. 7. Total electronic density of states of a) HAGNR-Pt, and b) NAGNR-Pt with and without the H_2S gas.

upon the adsorption of H_2S on the surface of NAGNR as shown in Fig. 6 (b). Furthermore, the density of states at Fermi level is zero for the cases of HAGNR as well as HAGNR-H_2S systems confirming the band structure results. Meanwhile, two small peaks are observed close to Fermi level around −0.15 and 0.21 eV for the cases of NAGNR and NAGNR-H_2S, which is also in agreement with the small band gap obtained from the band structure results. After doping the two HAGNR and NAGNR systems with Pt, the changes of electronic density of states after gas adsorption become more significant which verifies the band structure results. For instance, a shift to higher energy level is observed for the two cases of HAGNR-Pt and NAGNR-Pt upon the interaction with H_2S as shown in Fig. 7(a) and (b). Moreover, some other remarkable changes in the intensities of the peaks in the ranges of −10.1 to −1.4 eV in the valence band and 0.8–16.3 eV in the conduction band are observed for the case of HAGNR-Pt after gas adsorption. For the case of NAGNR-Pt, in addition to the shift to higher levels, a considerable increase in the DOS in the range of 0.7–17.4 eV in the conduction band is observed as well upon the adsorption of H_2S. The changes that appear in the electronic density of states of any of the developed HAGNR, NAGNR, HAGNR-Pt, and NAGNR-Pt systems after gas adsorption is an indication of variation in the available number of states of these systems upon gas adsorption [39]. These results reveal that the H_2S gas is adsorbed successfully on the surface of the four developed HAGNR, NAGNR, HAGNR-Pt, and NAGNR-Pt systems.

The I(V) analysis have been performed to study the influence of Pt-doping as well as the adsorption of H_2S on the conductivity of NAGNR system. As shown in Fig. 8(a), the current of NAGNR decreases after doping with Pt metal. Furthermore, upon adsorption of H_2S on the surface of NAGNR, no remarkable variations in the current are observed. Meanwhile, the current relatively increases upon gas adsorption on NAGNR-Pt. Those observations are consistent with the obtained band gap results in Fig. 5. The electrical response is an important parameter to evaluate the sensing capability of the developed sensors to the target gas. The response of a sensor is evaluated from the I(V) curves at a fixed voltage. Hence, the response (R (%)) of H_2S for the developed HAGNR, NAGNR, HAGNR-Pt, and NAGNR-Pt sensor materials is investigated using Eq. (3) [40]:

$$R\ (\%) = \left|\frac{I - I_o}{I_o}\right| x100 \tag{3}$$

Where I is the current of the proposed sensors with gas, and I_o is the current of any of the proposed sensors without H_2S gas. As shown in Fig. 8(b), the highest response of H_2S is observed for the cases of HAGNR-Pt and NAGNR-Pt sensor materials with 46.7 and 40.0 %, respectively. These results indicate that doping HAGNR and NAGNR with Pt play a crucial role in improving their sensing performance, which is in good agreement with the adsorption energy results shown in Table 1. The reason of improving the sensing performance is that doping graphene based materials may increase their specific surface area and hence facilitate their interaction with the target gas [41]. Specifically, it has been reported that doping with metals can increase remarkably the surface reactivity through supplying extra negative charges to the delocalized π systems due to the smaller electronegativity of platinum as compared with carbon [33]. Eventually, the adsorption energy as well as the adsorption length results of the current study are compared with the

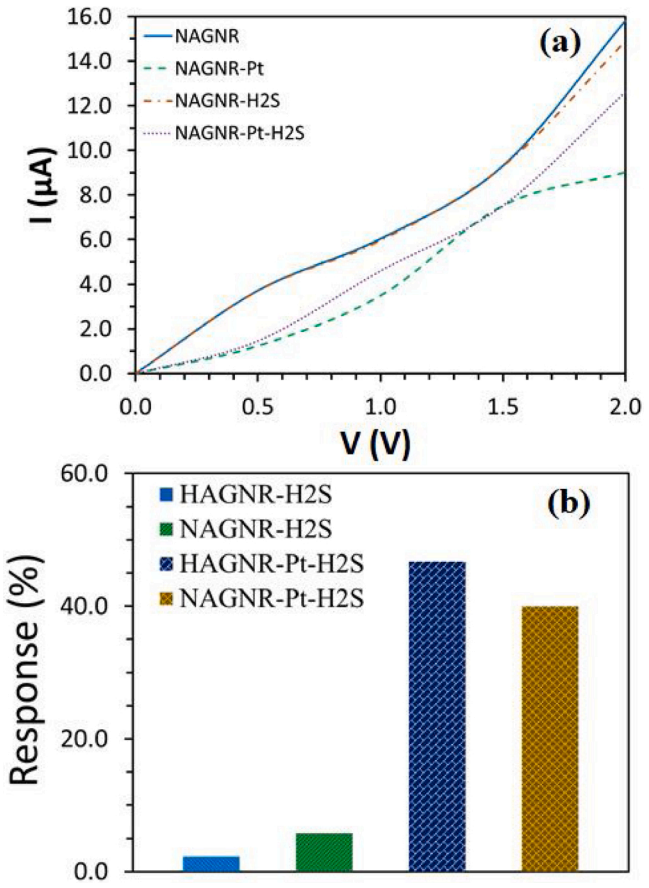

Fig. 8. a) I (V) curves of NAGNR and NAGNR-Pt systems with and without H_2S. (b) Electrical response for the H_2S gas of the developed HAGNR, NAGNR, HAGNR-Pt, and NAGNR-Pt sensors.

Table 2
Comparison between the adsorption energy and adsorption length results for H_2S adsorbed on different systems and the results achieved in the current investigation.

System	E_{ads} (eV)	D (Å)	Reference
Carbon nitride (C3N)	0.610	–	
C3N-C	2.843	1.759	[42]
C3N-N	1.581	3.489	
Pristine CNT	0.802	3.207	
B-CNT	0.608	2.922	[43]
N-CNT	0.788	3.223	
P-SiNR	−0.640	2.450	
N-SiNR	−1.860	2.400	[44]
B-SiNR	−0.900	1.980	
Pt-graphene	1.858	2.353	[15]
ZGNR	− 0.159	3.36	[45]
AGNR	− 0.269	3.50	
HAGNR-Pt	− 4.115	2.93	Current work
NAGNR-Pt	− 3.892	3.47	

results of the adsorption of H_2S gas on various systems as shown in Table 2. The results reveal that the adsorption energies of H_2S adsorbed on both HAGNR-Pt and NAGNR-Pt systems of the present work are remarkably high when compared with some of the recent reports.

4. Conclusion

In the present work, theoretical investigations for detection of the highly toxic H_2S gas using armchair graphene nanoribbon (AGNR) sensor materials were presented. The influence of terminating AGNR with hydrogen and nitrogen (HAGNR and NAGNR) as well as the effect of doping with Pt (HAGNR-Pt and NAGNR-Pt) on the sensing performance toward H_2S have been studied. The adsorption energy and the charge transfer between the gas and HAGNR were found to be −0.301 eV and −0.024 e, and −0.369 eV and −0.034 e for the case of NAGNR. The adsorption energy and the response of the developed HAGNR and NAGNR increased considerably after doping with Pt. More precisely, the adsorption energy increased to −4.115 and −3.892 eV for the cases of HAGNR-Pt and NAGNR-Pt, respectively. In addition, the highest response of H_2S gas was observed for the cases of HAGNR-Pt and NAGNR-Pt with 46.7 and 40.0 %, respectively. The obtained results of the adsorption energies in the current study indicate that H_2S gas was physisorbed on HAGNR and NAGNR, while it was chemisorbed on HAGNR-Pt and NAGNR-Pt. The investigation results suggest that the HAGNR-Pt and NAGNR-Pt sensor systems might be nominated as sensitive gas sensor materials to detect H_2S gas.

Declaration of Competing Interest

The authors declare that they have no known competing financial interests or personal relationships that could have appeared to influence the work reported in this paper.

Acknowledgements

The publication of this article was funded by the Qatar National Library.

References

[1] T.W. Lambert, V.M. Goodwin, D. Stefani, L. Strosher, Hydrogen sulfide (H2S) and sour gas effects on the eye. A historical perspective, Sci. Total Environ. 367 (2006) 1–22.
[2] M.D. Ganji, N. Danesh, Adsorption of H 2 S molecules by cucurbit [7] uril: an ab initio vdW-DF study, RSC Adv. 3 (2013) 22031–22038.
[3] B. Dai, C.M. Jones, M. Pearl, M. Pelletier, M. Myrick, Hydrogen sulfide gas detection via multivariate optical computing, Sensors 18 (2018) 2006.
[4] T. Bandosz, Q. Le, Evaluation of surface properties of exhausted carbons used as H2S adsorbents in sewage treatment plants, Carbon 36 (1998) 39–44.
[5] U. Shefa, M.-S. Kim, N.Y. Jeong, J. Jung, Antioxidant and cell-signaling functions of hydrogen sulfide in the central nervous system, Oxid. Med. Cell. Longev. 2018 (2018), 1873962.
[6] M. Lashgari, M. Ghanimati, Photocatalytic degradation of H2S aqueous media using sulfide nanostructured solid-solution solar-energy-materials to produce hydrogen fuel, J. Hazard. Mater. 345 (2018) 10–17.
[7] A.I. Ayesh, R.E. Ahmed, M.A. Al-Rashid, R.A. Alarrouqi, B. Saleh, T. Abdulrehman, Y. Haik, L.A. Al-Sulaiti, Selective gas sensors using graphene and CuO nanorods, Sens. Actuators A Phys. 283 (2018) 107–112.
[8] A.F. Abu-Hani, Y.E. Greish, S.T. Mahmoud, F. Awwad, A.I. Ayesh, Low-temperature and fast response H2S gas sensor using semiconducting chitosan film, Sens. Actuators B Chem. 253 (2017) 677–684.
[9] A.I. Ayesh, A.F. Abu-Hani, S.T. Mahmoud, Y. Haik, Selective H2S sensor based on CuO nanoparticles embedded in organic membranes, Sens. Actuators B Chem. 231 (2016) 593–600.
[10] O. Ovsianytskyi, Y.-S. Nam, O. Tsymbalenko, P.-T. Lan, M.-W. Moon, K.-B. Lee, Highly sensitive chemiresistive H2S gas sensor based on graphene decorated with Ag nanoparticles and charged impurities, Sens. Actuators B Chem. 257 (2018) 278–285.
[11] N. Van Hoang, C.M. Hung, N.D. Hoa, N. Van Duy, I. Park, N. Van Hieu, Excellent detection of H2S gas at ppb concentrations using ZnFe2O4 nanofibers loaded with reduced graphene oxide, Sens. Actuators B Chem. 282 (2019) 876–884.
[12] Z. Song, Z. Wei, B. Wang, Z. Luo, S. Xu, W. Zhang, H. Yu, M. Li, Z. Huang, J. Zang, Sensitive room-temperature H2S gas sensors employing SnO2 quantum wire/reduced graphene oxide nanocomposites, Chem. Mater. 28 (2016) 1205–1212.
[13] D. Cortés-Arriagada, N. Villegas-Escobar, D.E. Ortega, Fe-doped graphene nanosheet as an adsorption platform of harmful gas molecules (CO, CO2, SO2 and H2S), and the co-adsorption in O2 environments, Appl. Surf. Sci. 427 (2018) 227–236.
[14] X. Gao, Q. Zhou, J. Wang, L. Xu, W. Zeng, Performance of Intrinsic and Modified Graphene for the Adsorption of H2S and CH4: A DFT Study, Nanomaterials 10 (2020) 299.
[15] Z. Bo, X. Guo, X. Wei, H. Yang, J. Yan, K. Cen, Density functional theory calculations of NO2 and H2S adsorption on the group 10 transition metal (Ni, Pd and Pt) decorated graphene, Physica E Low. Syst. Nanostruct. 109 (2019) 156–163.
[16] S. Shanmugam, S. Nachimuthu, V. Subramaniam, DFT study of adsorption of ions on doped and defective graphene, Mater. Today Commun. 22 (2020), 100714.

[17] J. Liu, T. Liang, F. Wang, W. Lai, Y. Liu, Theoretical investigation of the catalytic and inhibiting role of boron in graphene oxidation, Mater. Today Commun. 23 (2020), 100885.
[18] E. Salih, A.I. Ayesh, Pt-doped armchair graphene nanoribbon as a promising gas sensor for CO and CO2: DFT study, Physica E Low. Syst. Nanostruct. 125 (2020), 114418.
[19] K.K. Paulla, A.A. Farajian, Concentration effects of carbon oxides on sensing by graphene nanoribbons: ab initio modeling, J. Phys. Chem. C 117 (2013) 12815–12825.
[20] N.K. Jaiswal, G. Kovačević, B. Pivac, Reconstructed graphene nanoribbon as a sensor for nitrogen based molecules, Appl. Surf. Sci. 357 (2015) 55–59.
[21] P. Orsu, A. Koyyada, Recent progresses and challenges in graphene based nano materials for advanced therapeutical applications: a comprehensive review, Mater. Today Commun. 22 (2020), 100823.
[22] E. Engel, R.M. Dreizler, Density Functional Theory, Springer, 2013.
[23] J.P. Perdew, K. Burke, M. Ernzerhof, Generalized gradient approximation made simple, Phys. Rev. Lett. 77 (1996) 3865.
[24] S. Grimme, Semiempirical GGA-type density functional constructed with a long-range dispersion correction, J. Comput. Chem. 27 (2006) 1787–1799.
[25] D.C. Liu, J. Nocedal, On the limited memory BFGS method for large scale optimization, Math. Program. 45 (1989) 503–528.
[26] E. Salih, A.I. Ayesh, Enhancing the sensing performance of zigzag graphene nanoribbon to detect NO, NO2, and NH3 gases, Sensors 20 (2020) 3932.
[27] W. Gao, P. Xiao, G. Henkelman, K.M. Liechti, R. Huang, Interfacial adhesion between graphene and silicon dioxide by density functional theory with van der Waals corrections, J. Phys. D Appl. Phys. 47 (2014), 255301.
[28] Y. Gui, Z. Hao, X. Li, C. Tang, L. Xu, Gas sensing of graphene and graphene oxide nanoplatelets to ClO2 and its decomposed species, Superlattices Microstruct. 135 (2019), 106248.
[29] E. Salih, A.I. Ayesh, First principle investigation of H2Se, H2Te and PH3 sensing based on graphene oxide, Phys. Lett. A 384 (2020), 126775.
[30] E. Salih, A.I. Ayesh, CO, CO2, and SO2 detection based on functionalized graphene nanoribbons: First principles study, Physica E Low. Syst. Nanostruct. 123 (2020), 114220.
[31] R. Carbó-Dorca, P. Bultinck, Quantum mechanical basis for Mulliken population analysis, J. Math. Chem. 36 (2004) 231–239.
[32] T. Kawai, Y. Miyamoto, O. Sugino, Y. Koga, Graphitic ribbons without hydrogen-termination: electronic structures and stabilities, Phys. Rev. B 62 (2000), R16349.
[33] Z. Khodadadi, Evaluation of H2S sensing characteristics of metals–doped graphene and metals-decorated graphene: insights from DFT study, Physica E Low. Syst. Nanostruct. 99 (2018) 261–268.
[34] E. Salih, A.I. Ayesh, DFT investigation of H2S adsorption on graphenenanosheets and nanoribbons: comparative study, Superlattices Microstruct. 146 (2020), 106650.
[35] T. Pakornchote, A. Ektarawong, B. Alling, U. Pinsook, S. Tancharakorn, W. Busayaporn, T. Bovornratanaraks, Phase stabilities and vibrational analysis of hydrogenated diamondized bilayer graphenes: a first principles investigation, Carbon 146 (2019) 468–475.
[36] M.G. Ahangari, A.H. Mashhadzadeh, M. Fathalian, A. Dadrasi, Y. Rostamiyan, A. Mallahi, Effect of various defects on mechanical and electronic properties of zinc-oxide graphene-like structure: a DFT study, Vacuum 165 (2019) 26–34.
[37] X. Gao, Q. Zhou, J. Wang, L. Xu, W. Zeng, Adsorption of SO2 molecule on Ni-doped and Pd-doped graphene based on first-principle study, Appl. Surf. Sci. 517 (2020), 146180.
[38] V.E.C. Padilla, M.T.R. de la Cruz, Y.E.Á. Alvarado, R.G. Díaz, C.E.R. García, G. H. Cocoletzi, Studies of hydrogen sulfide and ammonia adsorption on P-and Si-doped graphene: density functional theory calculations, J. Mol. Model. 25 (2019) 94.
[39] G.K. Walia, D.K.K. Randhawa, First-principles investigation on defect-induced silicene nanoribbons—a superior media for sensing NH3, NO2 and NO gas molecules, Surf. Sci. 670 (2018) 33–43.
[40] A.I. Ayesh, A.A. Alyafei, R.S. Anjum, R.M. Mohamed, M.B. Abuharb, B. Salah, M. El-Muraikhi, Production of sensitive gas sensors using CuO/SnO 2 nanoparticles, Appl. Phys. A 125 (2019) 550.
[41] X. Jia, H. Zhang, Z. Zhang, L. An, First-principles investigation of vacancy-defected graphene and Mn-doped graphene towards adsorption of H2S, Superlattices Microstruct. 134 (2019), 106235.
[42] O. Faye, U. Eduok, J.A. Szpunar, A.C. Beye, Two-dimensional carbon nitride (C3N) nanosheets as promising materials for H2S and NH3 elimination: a computational approach, Physica E Low. Syst. Nanostruct. 117 (2020), 113794.
[43] R. Srivastava, H. Suman, S. Shrivastava, A. Srivastava, DFT analysis of pristine and functionalized zigzag CNT: a case of H2S sensing, Chem. Phys. Lett. 731 (2019), 136575.
[44] S. Aghaei, M. Monshi, I. Calizo, A theoretical study of gas adsorption on silicene nanoribbons and its application in a highly sensitive molecule sensor, RSC Adv. 6 (2016) 94417–94428.
[45] H. Suman, R. Srivastava, S. Shrivastava, A. Srivastava, A. Jacob, C. Malvi, DFT analysis of H2S adsorbed zigzag and armchair graphene nanoribbons, Chem. Phys. Lett. 745 (2020), 137280.